

# Identifying septic shock subgroups to tailor fluid strategies through multi-omics integration

Received: 1 April 2024

Accepted: 7 October 2024

Published online: 19 October 2024



Zhongheng Zhang<sup>1,2,15</sup>✉, Lin Chen<sup>3,15</sup>, Bin Sun<sup>4</sup>, Zhanwei Ruan<sup>5</sup>, Pan Pan<sup>6</sup>, Weimin Zhang<sup>7</sup>, Xuandong Jiang<sup>7</sup>, Shaojiang Zheng<sup>8,9,15</sup>, Shaowen Cheng<sup>10,15</sup>, Lina Xian<sup>11</sup>, Bingshu Wang<sup>12</sup>, Jie Yang<sup>1</sup>, Bo Zhang<sup>1</sup>, Ping Xu<sup>13</sup>, Zhitao Zhong<sup>13</sup>, Lingxia Cheng<sup>13</sup>, Hongying Ni<sup>14</sup>, the Chinese Multi-omics Advances In Sepsis (CMAISE) Consortium\* & Yucai Hong<sup>1</sup>

Fluid management remains a critical challenge in the treatment of septic shock, with individualized approaches lacking. This study aims to develop a statistical model based on transcriptomics to identify subgroups of septic shock patients with varied responses to fluid strategy. The study encompasses 494 septic shock patients. A benefit score is derived from the transcriptome space, with higher values indicating greater benefits from restrictive fluid strategy. Adherence to the recommended strategy is associated with a hazard ratio of 0.82 (95% confidence interval: 0.64–0.92). When applied to the baseline hospital mortality rate of 16%, adherence to the recommended fluid strategy could potentially lower this rate to 13%. A proteomic signature comprising six proteins is developed to predict the benefit score, yielding an area under the curve of 0.802 (95% confidence interval: 0.752–0.846) in classifying patients who may benefit from a restrictive strategy. In this work, we develop a proteomic signature with potential utility in guiding fluid strategy for septic shock patients.

Intravenous fluid resuscitation is a widely employed therapy during the management of patients experiencing septic shock. The primary objective of this therapy is to replenish or enhance intravascular volume, which is often depleted or compromised in sepsis due to vasodilation of the vascular network<sup>1,2</sup>. This approach aims to improve both macrovascular perfusion, such as stroke volume and cardiac output, and microvascular perfusion, including capillary blood flow, thereby addressing organ hypoperfusion—a key aspect of sepsis pathophysiology that guides resuscitation efforts<sup>3</sup>. However, intravenous fluid resuscitation may lead to dilutional coagulopathy, fluid overload, and pathological edema in various organs, particularly the lungs<sup>4,5</sup>. Additionally, vasopressor agents are frequently utilized to address hypoperfusion by inducing constriction of arterioles and venules while enhancing cardiac contractility. Nonetheless,

vasopressor therapy carries inherent risks, such as vasoconstriction-associated tissue ischemia, elevated cardiac workload, and potential arrhythmias. Clinicians have historically combined these two therapeutic modalities to deliver supportive care to individuals with sepsis-related hypoperfusion. However, there remains a scarcity of data guiding the precise administration of intravenous fluids or vasopressors in the management of septic shock. Current resuscitation practices in patients with septic shock exhibit variability, ranging from restricted volume and early vasopressor administration to liberal fluid administration and delayed vasopressor initiation<sup>6</sup>.

Numerous clinical trials have been conducted to investigate the efficacy of liberal vs restrictive fluid strategies, employing diverse fluid administration protocols<sup>7–13</sup>. However, these studies have not consistently demonstrated the superiority of either strategy<sup>14</sup>. Septic

A full list of affiliations appears at the end of the paper. \*A list of authors and their affiliations appears at the end of the paper.

✉ e-mail: [zh\\_zhang1984@zju.edu.cn](mailto:zh_zhang1984@zju.edu.cn)

**Table 1 | Baseline characteristics of subjects in the training and validation cohorts**

Variables	Total, (n = 494)	Training cohort, (n = 352)	Validation cohort, (n = 142)	p
Age, median (Q1, Q3)	71 (60, 81)	71 (59, 81)	72 (64, 82)	0.173
Sex, male (%)	313 (63)	224 (64)	89 (63)	0.922
Height (cm), Median (Q1, Q3)	165 (158, 171)	165 (158, 172)	165 (158, 170)	0.275
Weight (kg), Median (Q1, Q3)	60 (55, 70)	60 (55, 70)	60 (54, 69.25)	0.502
Infection site, n (%)				<0.001
Abdomen	75 (15)	39 (11)	36 (25)	
Biliary/liver	54 (11)	31 (9)	23 (16)	
Brain	4 (1)	3 (1)	1 (1)	
Intestine	26 (5)	16 (5)	10 (7)	
Lung/chest	186 (38)	146 (41)	40 (28)	
Others	51 (10)	44 (12)	7 (5)	
Soft tissue	20 (4)	18 (5)	2 (1)	
Urinary	78 (16)	55 (16)	23 (16)	
SOFA, median (Q1, Q3)	9 (7, 12)	9 (7, 12)	9.5 (7, 12)	0.179
CRP (mg/dl), median (Q1, Q3)	140.52 (64.5, 217.03)	138.75 (63.97, 211.08)	147.31 (72.62, 238.12)	0.406
Lactate (mmol/L), median (Q1, Q3)	3 (1.9, 5)	2.67 (1.7, 4.52)	3.55 (2.42, 6.2)	<0.001
Fluid intake (ml/day), median (Q1, Q3)	3045 (1980, 4455.3)	2950 (1917, 4310)	3306.5 (2044.25, 4956.75)	0.081
Urine (ml/day), median (Q1, Q3)	1000 (377.5, 1862.5)	1027.5 (427.5, 1950)	850 (303.75, 1667.5)	0.063
Mortality, n (%)	79 (16)	64 (18)	15 (11)	0.051
Hospital days, median (Q1, Q3)	13.27 (9, 23.53)	13.54 (9, 24)	13 (8.05, 22)	0.404

Two-sided *p*-values are reported.  
Q1 first quartile, Q3 third quartile, SOFA sequential organ failure assessment, CRP C-reactive protein.

shock encompasses a heterogeneous patient population, suggesting that distinct subgroups may exhibit disparate responses to a given fluid strategy<sup>1,15</sup>. Therefore, precise management of septic shock holds promise for uncovering insights into fluid strategies. A multi-omics study involves integrating and analyzing data from various omics disciplines, including genomics, transcriptomics, proteomics, metabolomics, and epigenomics. By amalgamating information from multiple omics layers, researchers can achieve a more comprehensive understanding of biological systems and processes of sepsis<sup>16–18</sup>. Fluid administration can impact various biological systems, such as coagulation, endothelial function, electrolyte balance, and inflammatory responses. Thus, employing systems biology approaches to identify subgroups of septic shock patients may offer new insights into the effectiveness of fluid strategies. In this work, we identify septic shock patient subgroups with differential responses to fluid strategies and develop a proteomic signature for predicting group membership. Ultimately, this research lays the foundation for precise fluid management in patients with septic shock.

**Results**  
**Study population**

The study included a total of 494 patients diagnosed with septic shock, contributing to 1285 person-days, with 352 patients in the training cohort (Table 1). The validation cohort, consisting of 142 patients, was sourced from independent hospitals distinct from those contributing to the training set (Fig. 1). The treatment provided was consistent with the usual care at the respective hospitals, and no specific intervention was introduced by the study protocol. Both cohorts exhibited similar baseline characteristics, encompassing age, sex, height, weight, sequential organ failure assessment (SOFA) scores, mortality rates, and length of hospital stays. However, differences were noted in terms of infection site and serum lactate levels between the two cohorts. In the training cohort, 255 patients received a liberal fluid strategy, while 97 received a restrictive fluid strategy on day 1 (Supplementary Table 1). Patients assigned to the restrictive strategy group presented with

more severe illness (SOFA score = 10 [8, 12] vs 8 [6.5, 11], *p* < 0.001), a higher mortality rate (24% vs 16%), and increased vasopressor dosages. Additionally, patients in the restrictive strategy group had significantly lower fluid intake (2110 [1556.7, 2569] ml vs 3448.1 [2504, 4820.8] ml/day, *p* < 0.001) and reduced urine output (815 [285, 1587.5] vs 1100 [505, 2373.75] ml/day; *p* = 0.007).

**Subgroup identification**

In our study, we comprehensively quantified 61,792 genes across all samples before applying our filtering criteria, including both protein-coding and non-protein-coding genes. For a detailed description of our methodology, including library preparation, sequencing specifications, alignment and quantification techniques, and filtering criteria, please refer to the supplemental methods provided. Genes with a total expression count of less than 100 across all samples were filtered out. This criterion was chosen to ensure that we focus our analysis on genes with sufficient overall expression to provide reliable statistical power, while minimizing the inclusion of genes with very low expression, which might introduce noise and reduce the robustness of our findings. There was overlap of the propensity score between the liberal and restrictive groups (Supplementary Fig. 1). Utilizing LASSO with cross-validation criterion, 13 genes were identified to interact with treatment effects, namely *DEFA8P*, *ENSG00000255641*, *ENSG00000262304*, *ENSG00000264063*, *ENSG00000284292*, *ENSG00000285238*, *ENSG00000289707*, *FAM220A*, *FARP1*, *HLA-J*, *HNRNPUL2-BSCL2*, *IFNG-AS1*, *KLRC4*, *LY75-CD302*, and *PAQR9* (Supplementary Figs. 2 and 3). Analysis of the training dataset revealed that patients with congruent recommended and administered fluid strategies experienced significantly improved survival outcomes compared to those with disparate strategies (Supplementary Table 2 and Fig. 2). In particular, the Liberal.Restrict group had the worst survival outcome (Fig. 2 and Table 2). The treatment effects, conditioned on recommended subgroups, yielded mean differences in survival days of 59.7 days (estimate of  $E[Y|T=liberal, recom=liberal] - E[Y|T=restrictive, recom=liberal]$ ) and 41.7 days (estimate

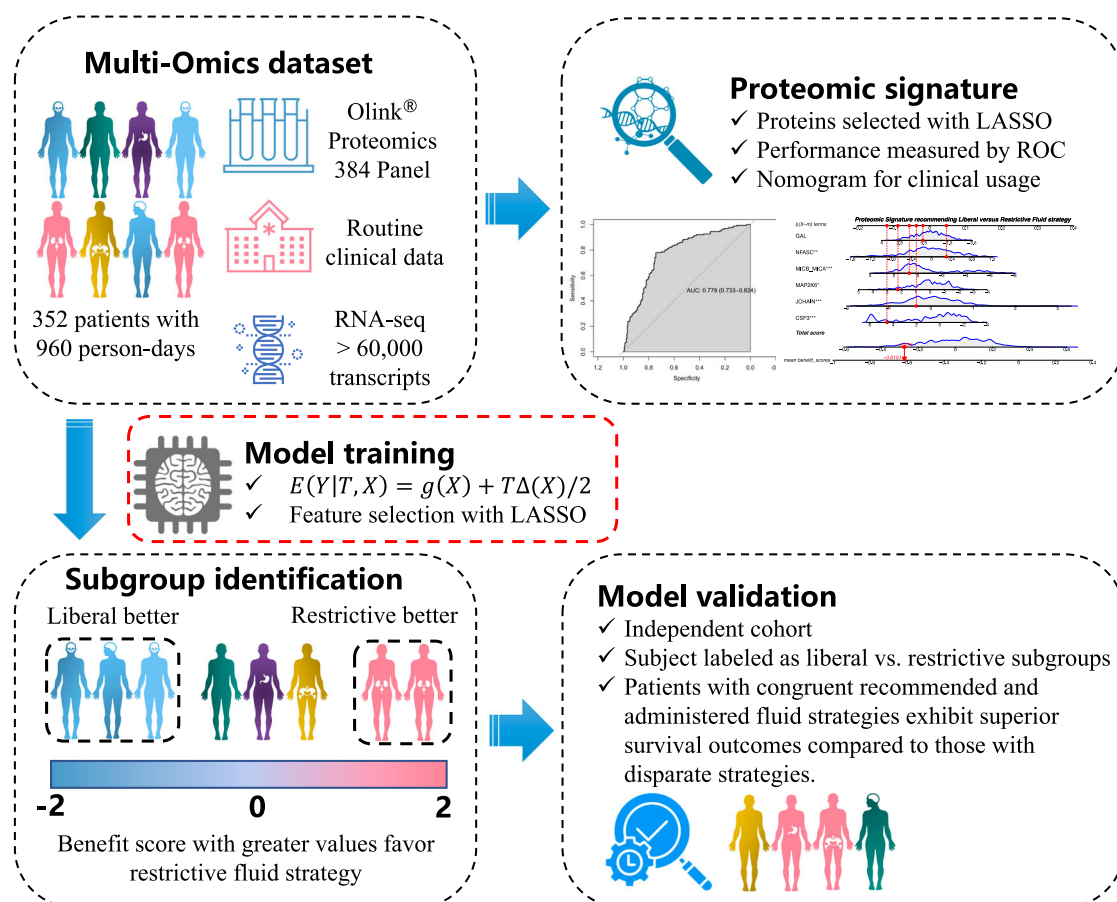


**Fig. 1 | An overview of the analysis workflow of the study.** The workflow involved four steps: construction of a multi-omics dataset, subgroup identification, model validation in an independent cohort, and development of a proteomic signature.

LASSO least absolute shrinkage and selection operator, ROC receiver operating characteristics, AUC area under curve, RNA-seq ribonucleic acid sequencing.

of  $E[Y|T = \text{restrictive}, \text{recom} = \text{restrictive}] - E[Y|T = \text{liberal}, \text{recom} = \text{restrictive}]$  for liberal and restrictive fluid strategies, respectively. The benefit score spanned from -1.75 to 1.21, with higher values indicative of a more favorable outcome with the restrictive strategy. In the validation cohort, these metrics were 48.1 and 19.4 days for groups recommending liberal and restrictive fluid strategies, respectively (Supplementary Fig. 4). On average, there was an increase of 19.9 days in time-to-event if all patients adhered to the fluid strategy recommended by the benefit score. This effect corresponds to a hazard ratio of 0.82 (95% confidence interval (CI): 0.64–0.92). When applied to the baseline reference hospital mortality rate of 16%, adherence to the recommended fluid strategy could potentially lower this rate to 13%.

Supplementary Table 3 presents the clinical disparities between recommended liberal and restrictive fluid strategy groups. Figure 3a illustrates the nuanced clinical differences among groups that recommended different fluid strategies. It is observed that patients predicted to benefit from restrictive fluid resuscitation predominantly presented with more severe pulmonary and renal injuries, indicated by higher  $\text{FiO}_2$  requirements. Despite minimal clinical feature space separation between the restrictive and liberal groups, as depicted in Fig. 3b, a pronounced distinction was noted in the transcriptomic space, as shown in Fig. 3c.

Given the importance of reconciling the gap between recommended and actual treatment, we categorized patients into four distinct groups based on the fluid strategies that were recommended and those that were ultimately administered. Despite no significant differences in commonly recorded clinical features, suggesting limitations in using routine variables for fluid strategy prescription, further

comparison of clinical variables revealed significantly higher urine output in the liberal-liberal group and elevated SOFA score in the restrictive-restrictive group (Supplementary Fig. 5). While the recommended restrictive and liberal groups exhibited minimal separation in the clinical feature space (Supplementary Fig. 6), greater distinctiveness was observed in the transcriptomic space (Supplementary Fig. 7). Over the course of sepsis from day 1 to 5, a trend towards recommending restrictive fluid strategy emerged (Supplementary Fig. 8). In our study, we observed distinct gene expression profiles between patients who benefited from restrictive vs liberal fluid strategies. For instance, higher expressions of *CLDN8*, *TPO*, *DIO2*, and *IYD*, were associated with better outcomes in the restrictive fluid group. Claudin proteins are components of tight junctions in epithelial and endothelial cells. *CLDN8* specifically has been implicated in the regulation of vascular permeability<sup>19,20</sup>, making it a candidate gene that could be associated with vascular endothelial dysfunction in sepsis. *DIO2* and *IYD* are involved in the activation of thyroid hormones. Thyroid hormones can influence the cardiovascular system, including endothelial function<sup>21,22</sup>. Figure 4 offers a sophisticated molecular dissection of the responses to restrictive and liberal fluid strategies in sepsis. The differential gene expression analysis (Fig. 4a) elucidates the molecular divergence between patients potentially benefiting from restrictive vs liberal fluid strategies. The enrichment analysis reveals a notable modulation of biological processes related to sensory perception and neurotransmission (Fig. 4b). This indicates that fluid strategy may exert neuromodulatory effects, influencing pathways that could be implicated in the neuroinflammatory sequelae of sepsis, including cognitive impairment and pain perception alterations. Further

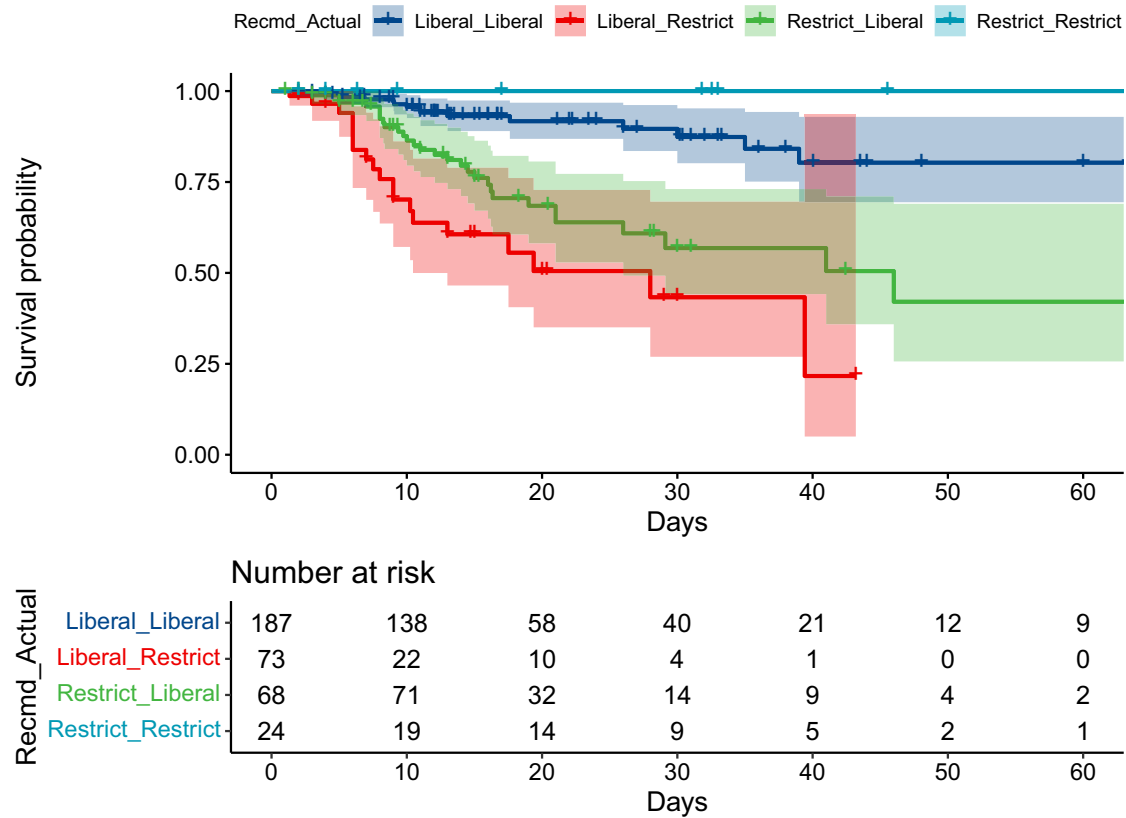


**Fig. 2 | Survival curves stratified by the recommended and received subgroups, with the shaded area indicating the 95% CI.** Groups are denoted as “Recmd\_Actual,” where, for instance, “Liberal\_Restrict” signifies a recommendation for a liberal fluid strategy but actual receipt of a restrictive one. Censored patients are denoted by small “+” symbols. Data are presented as mean values and a 95% CI.

examination of metabolic pathways uncovers perturbations in fundamental metabolic processes, including glycolysis and cholesterol biosynthesis (Fig. 4c). These metabolic disturbances may reflect the body’s adaptive or maladaptive efforts to maintain energy homeostasis under the influence of different fluid management approaches. Figure 4d provides a deeper exploration of the immunological and hematological responses. The observed enrichment of pathways related to platelet activation and immunoglobulin production suggests a differential impact on hemostasis and the humoral immune response.

**Table 2 | Cox proportional model incorporating time-varying covariates**

Variables	HR [95% CI]	p
Recmd_Actual: Liberal_Liberal	Reference	
Recmd_Actual: Liberal_Restrict	5.00 [2.40, 10.44]	<0.001
Recmd_Actual: Restrict_Liberal	3.50 [1.87, 6.54]	<0.001
Recmd_Actual: Restrict_Restrict	0.91 [0.82, 1.53]	0.996
Age (for each 1-year increase)	1.02 [1.00, 1.04]	0.049
SOFA (for each 1-point increase)	1.07 [1.00, 1.15]	0.065
Lactate (for each 1 mmol/l increase)	1.26 [1.17, 1.36]	<0.001

Recmd\_Actual: in this study, patients underwent categorization into four distinct groups according to the fluid strategy either recommended or actually administered. For instance, the classification “Liberal\_Liberal” denotes that a patient received a liberal fluid strategy as per actual treatment, with the algorithm also recommending the same strategy. Similarly, “Liberal\_Restrict” indicates that although the patient is currently undergoing a restrictive fluid strategy, the algorithm suggested a liberal approach. Two-sided *p*-values are reported. SOFA sequential organ failure assessment, HR hazard ratio.

**Association of sepsis endotypes with the fluid resuscitation benefit score**

Sepsis endotypes were discerned through the application of the Partitioning Around Medoids (PAM) method, which evaluated gene expression profiles. The analysis revealed two distinct sepsis endotypes. Cluster 1 was distinguished by an exaggerated hyperinflammatory profile, whereas Cluster 2 was marked by a relative downregulation of pro-inflammatory cytokines (Fig. 5a), corroborating findings from existing literature<sup>18,23–25</sup>. The clustering outcomes were then integrated with the previously determined benefit scores, demonstrating that Cluster 2 patients potentially responded better to a restrictive fluid strategy (Fig. 5b). A significant differential expression was observed between the endotypes for a multitude of genes, encompassing both protein-coding and non-coding RNAs (Fig. 5c).

Functional enrichment analysis of these genes indicated their involvement in various immunological pathways, including leukocyte-mediated immunity, adaptive immune responses, immunoglobulin-mediated immune reactions, and T-cell activation (Fig. 5d). These biological pathways are pivotal in the immunopathogenesis of sepsis and may offer insights into the heterogeneity of treatment responses among different sepsis endotypes.

**Proteomic signature for recommending the fluid strategy**

We developed a proteomic signature to leverage the stability and direct biological relevance of proteins in the clinical setting, despite the close association of transcriptomic data with clinical outcomes. The proteomic approach facilitates rapid measurement with standard clinical assays, supporting practical application in sepsis management<sup>26</sup>. We evaluated 363 plasma proteins and conducted PCA to explore the variability and confounders (Fig. 6). The PCA revealed a



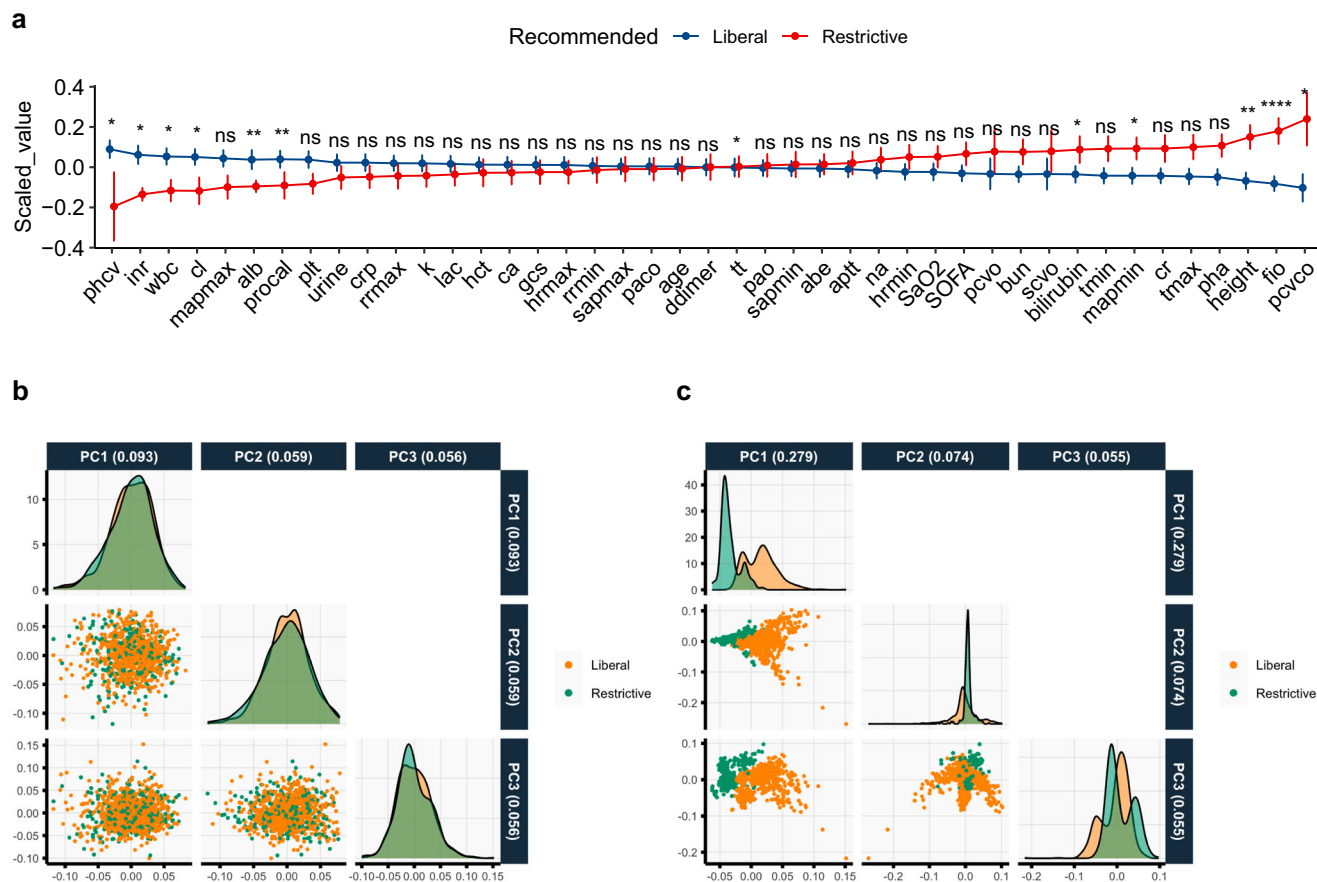


**Fig. 3 | Comparison of clinical and transcriptomic features between patients who may benefit from restrictive fluid strategy and those who may benefit from liberal strategy.** **a** The two groups, liberal ( $n = 260$ ) and restrictive ( $n = 92$ ), were compared for their differences in clinical features. Analysis of variance (ANOVA) was employed to assess the statistical differences in each variable represented on the x-axis across the four groups. Significance levels are indicated with asterisks as follows:  $p < 0.05$ ,  $^{**}p < 0.01$ , and  $^{***}p < 0.001$ . Data are presented as mean values  $\pm$  SEM, and it is noted that all variables have been normalized for comparison purposes. **b** A plot matrix is presented to illustrate the distribution of samples within the clinical feature space, as defined by the first three principal components. **c** Similarly, another plot matrix shows the distribution of samples within the transcriptomic feature space, also based on the first three principal components. *urine* Urine volume; *plt* platelet count, *pcvo* central venous oxygen saturation, *sapmin* minimum arterial lactate, *cl* creatinine level, *tmin* minimum

body temperature, *scvo* mixed venous oxygen saturation, *wbc* white blood cell count, *paco* arterial carbon dioxide pressure, *inr* international normalized ratio, *rrmax* maximum respiratory rate, *alb* albumin, *k* potassium, *mapmax* maximum mean arterial pressure, *ddimer* D-dimer, *hct* Hematocrit, *mapmin* minimum mean arterial pressure, *gcs* Glasgow coma scale, *pao* arterial oxygen pressure, *aptt* activated partial thromboplastin time, *lac* lactic acid, *SaO<sub>2</sub>* arterial oxygen saturation, *procal* procalcitonin, *phcv* pH of central venous blood, *na* sodium, *ca* calcium, *hrmax* maximum heart rate, *abe* base excess, *tt* thrombin time, *tmax* maximum body temperature, *crp* C-reactive protein, *sapmax* maximum arterial lactate, *age* age, *hrmin* minimum heart rate, *rrmin* minimum respiratory rate, *bilirubin* bilirubin, *height* height, *cr* creatinine clearance, *pha* pH value of arterial blood, *pcvo* carbon dioxide of central venous blood, *bun* blood urea nitrogen, *fio* fractional inspired oxygen, *SOFA* sequential organ failure assessment score, *scaled\_value* scaled value.

moderate distinction between survivors and non-survivors (Fig. 6a), no significant batch effects across hospital samples (Fig. 6b), and patients with elevated SOFA scores were clustered in the upper-left quadrant of the plot (Fig. 6c).

Differential expression analysis revealed significant differences between the restrictive and liberal fluid strategy groups, highlighting CSF3, MICB\_MICA, and CXCL9 (Fig. 7a). Gene set enrichment analysis (GSEA) indicated enrichment in pathways related to bacterial response, lipid cellular response, and steroid hormone response (Supplementary Fig. 9). Important biological pathways such as interleukin-10 signaling, regulation of hormone secretion, and response to oxygen-containing compounds were identified (Supplementary Fig. 10). Using a LASSO regression model against the benefit score, a proteomic signature comprising GAL, NFASC, MICB\_MICA, MAP2K6, JCHAIN, and CSF3 was derived (Table 3, Supplementary Fig. 11, and Fig. 7b). The six proteins, highlighted in Supplementary Table E4 and integral to our predictive nomogram, play pivotal roles in orchestrating immune responses and endothelial damage<sup>27,28</sup>. Despite

the current assays requiring 3–5 h to yield results, there is a pressing requirement for their optimization to expedite this process. Streamlining the assay timeline is crucial for the ICU setting, where the speed of clinical decision-making can influence patient outcomes. The performance of this model in recommending restrictive vs liberal fluid strategy yielded an area under the curve (AUC) of 0.802 (95% CI: 0.752 to 0.846; Fig. 7c), which was comparable to that developed by transcriptomic data (AUC = 0.845, 0.797–0.884). It is also noted that other machine learning models do not show significant improvement over the logistic regression model in classifying subgroups of patients who may benefit from a restrictive fluid strategy (Fig. 7c).

## Discussion

The study devised a benefit score based on transcriptomic data to guide fluid management in septic shock patients. This score ranged from  $-2$  to  $2$ , with higher values indicating potential benefits from a restrictive fluid strategy. The restrictive approach involved administering less fluid and early vasopressor use to maintain target blood

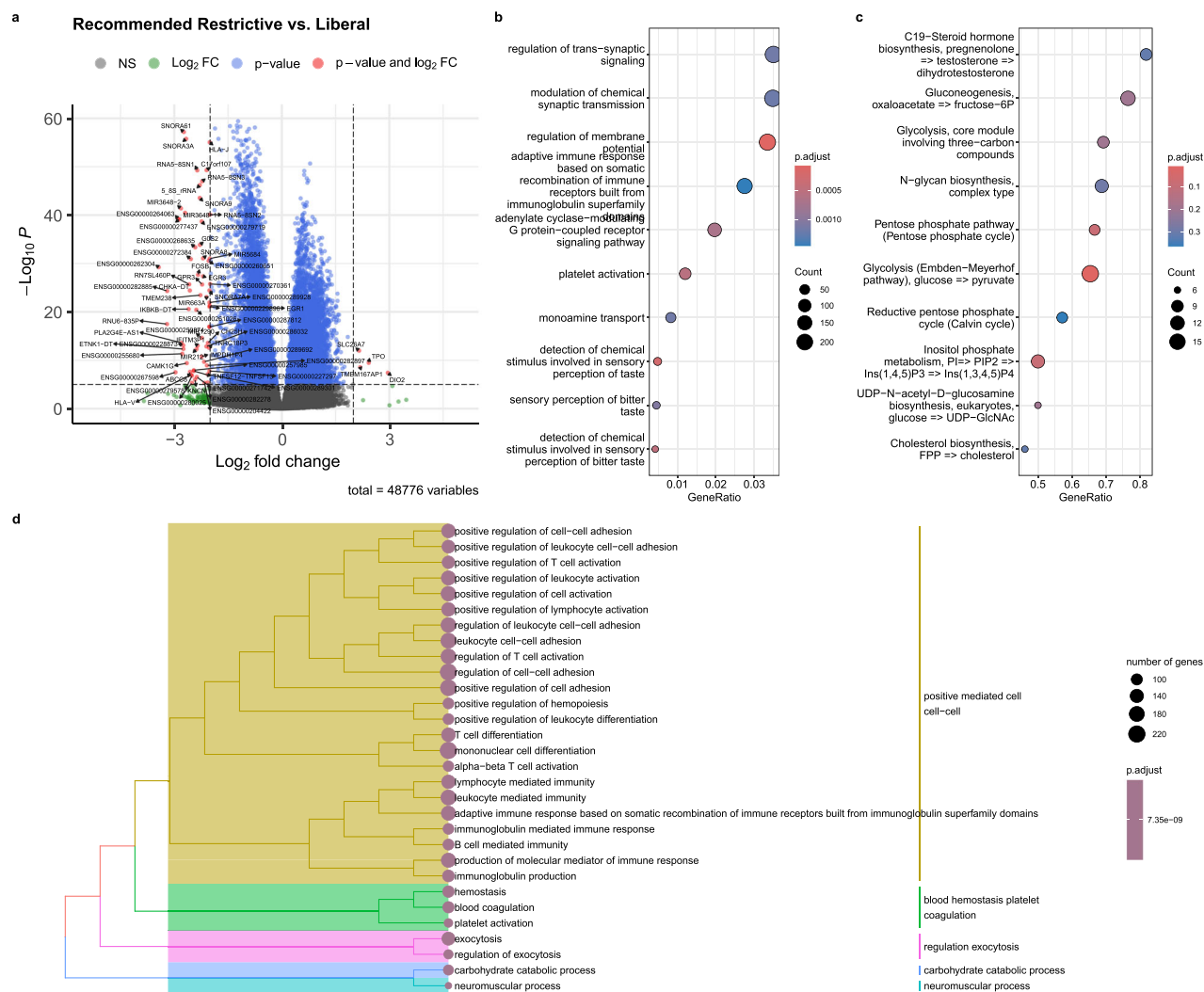


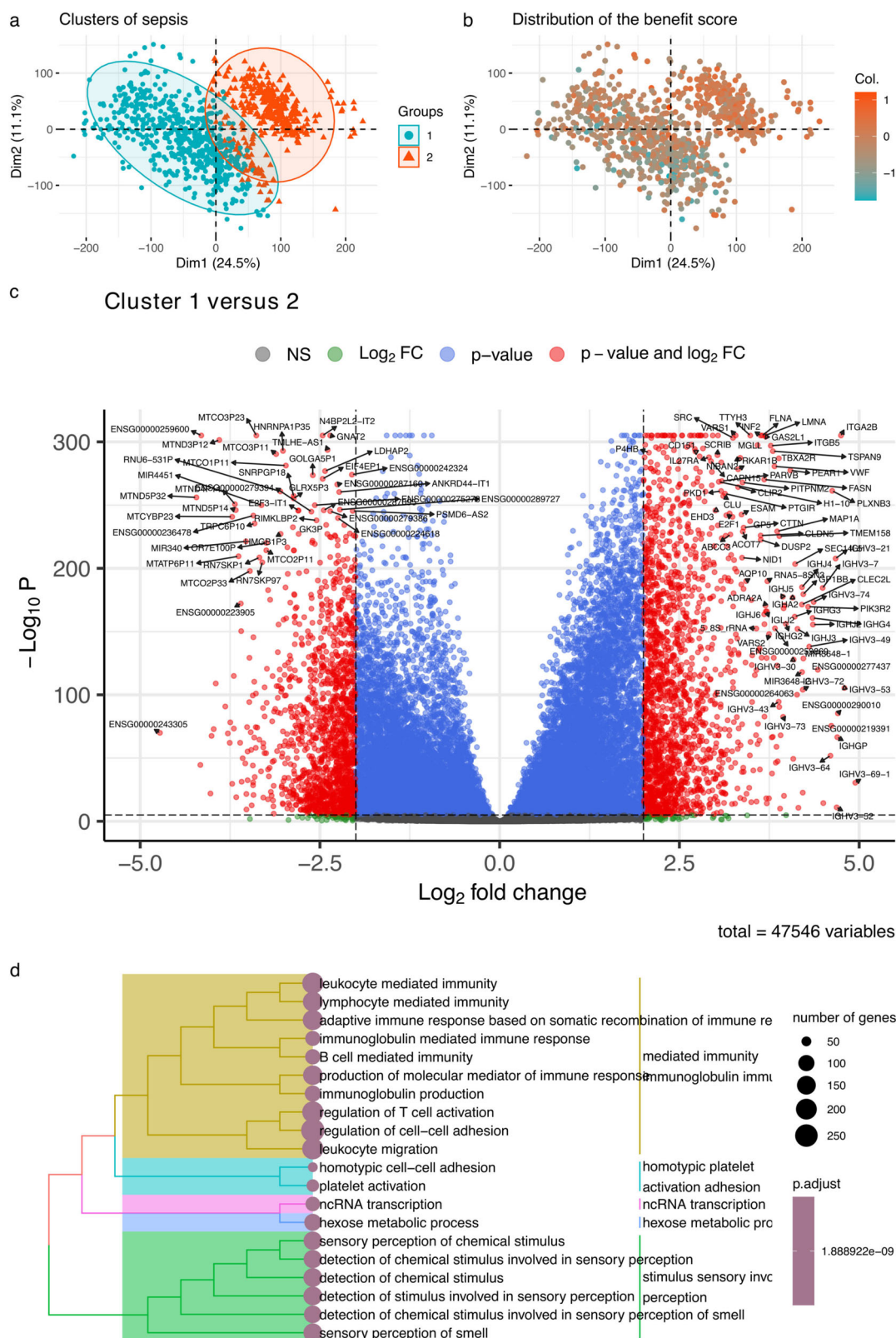
**Fig. 4 | Transcriptomic profiles of the recommended restrictive vs liberal fluid strategy groups.** **a** A volcano plot illustrates differentially expressed genes between restrictive and liberal fluid strategy groups. Positive values denote higher expression in the restrictive group than the liberal group. *p*-values were adjusted using the Benjamini–Hochberg procedure. **b** The dot plot displays gene ontology (GO) enrichment pathways for the differentially expressed genes. Adjusted two-sided *p*-values are indicated by color, while circle size represents gene count. **c** The dot plot exhibits Molecular Knowledge-based Kyoto Encyclopedia of Genes and Genomes (MKEGG) enrichment pathways for the differentially expressed genes. Adjusted two-sided *p*-values are depicted by color, with circle size indicating gene count. **d** A tree plot presents GO enrichment pathways for differentially expressed genes using gene set enrichment analysis (GSEA). Adjusted two-sided *p*-values are visualized by color, while circle size reflects gene count. MKEGG refers to the

“molecular knowledge-based” pathway database provided by the Kyoto Encyclopedia of Genes and Genomes (KEGG). This database contains curated information on molecular interactions, reactions, and pathways in various biological systems, including metabolic pathways, signaling pathways, and diseases. In the figure, Ensembl IDs and gene symbols are used. Some genes do not have official gene symbols because they were recently discovered or annotated and might not have been evaluated and approved. Some genomic elements, such as pseudogenes or certain types of non-coding RNA, may not be given symbols because they do not encode proteins or have known regulatory functions. For instance, the Ensembl ID ENSG00000264063 corresponds to an RNA gene that is specifically categorized under the class of microRNAs (miRNAs). As a non-coding RNA, it has not been assigned a conventional gene symbol.

pressure. Validation was conducted in an independent, non-overlapping cohort recruited from different hospitals during the same period as the training cohort. Due to the technical challenges associated with measuring RNA expression levels, a proteomic signature was further developed to facilitate clinical translation. Six proteins were identified from a pool of 363 plasma proteins. The proteomic signature demonstrated moderate performance in differentiating patients who might benefit from a restrictive fluid strategy. Additionally, a nomogram was devised to aid in the clinical application of the findings. Our study’s novelty lies in its comprehensive multimodal approach, offering a unique perspective on sepsis heterogeneity. By identifying a distinct proteomic signature associated with differential responses to fluid resuscitation, our work contributes to the

advancement of personalized sepsis management. This tailored approach has the potential to optimize treatment strategies, thereby enhancing clinical outcomes and addressing the unmet need for precision in septic shock therapy.

Numerous studies have investigated fluid management strategies in patients with septic shock or sepsis-induced hypotension<sup>9,12,29</sup>. Despite variations in protocols, these studies have not demonstrated the clear benefits of either restrictive or liberal fluid strategies<sup>29</sup>. We hypothesize that sepsis encompasses a heterogeneous population, with certain subgroups potentially benefiting from restrictive fluid strategies while others do not<sup>23,30–32</sup>. Previous attempts to identify patient subgroups using unsupervised machine learning algorithms have been limited by their inability to incorporate interventions, thus



hindering their ability to guide treatment decisions<sup>32</sup>. In our study, we introduced a benefit score designed to guide fluid management strategies. Unlike traditional approaches such as outcome modeling and unsupervised clustering, our method prioritizes modeling treatment-covariate interactions over main covariate effects. This emphasis stems from the fact that subgroup identification hinges solely on interaction signs<sup>33,34</sup>. The benefit score, introduced in our study,

quantifies the individualized treatment effect by capturing the magnitude of interaction. This score facilitates the recommendation of restrictive fluid strategies using varied cutoff values tailored to real clinical scenarios. By integrating interventions into causal inference models, we aim to comprehensively explore the interplay between treatment and covariates driving heterogeneity of main effects. Distinct gene expression patterns were observed among patients



**Fig. 5 | Identification of two sepsis endotypes in the transcriptomic space.**

**a** This panel provides a visualization of the sepsis endotypes in the space defined by the first two principal components. The clusters are differentiated by color and point shape, indicating the distinct transcriptomic profiles of each endotype. **b** The distribution of the benefit score within the PCA space is depicted, with the red color signifying patients who are more likely to benefit from a restrictive fluid strategy, and the blue color indicating those who may benefit from a liberal fluid strategy. **c** A volcano plot is presented to illustrate the differentially expressed genes between the two sepsis endotypes. Genes are identified using their Ensembl IDs and gene

symbols. It is noted that some genes, particularly those recently discovered or annotated, may not have official gene symbols. Additionally, certain genomic elements such as pseudogenes or specific types of non-coding RNA, which do not encode proteins or have established regulatory functions, may lack symbols. Adjusted two-sided *p*-values were reported. **d** A tree plot is utilized to present GO enrichment pathways for the differentially expressed genes, as determined by GSEA. The adjusted two-sided *p*-values are represented by color intensity, with the circle size corresponding to the count of genes within each pathway.

differentially responding to restrictive fluid strategies, with implicated genes participating in critical biological processes such as cell activation, membrane potential regulation, platelet activation, complement cascade, and cell–cell adhesion. In sepsis, the activation of immune cells, predominantly leukocytes, triggers the release of inflammatory mediators that impair endothelial function, leading to enhanced vascular permeability through the disruption of tight junctions and the glycocalyx layer. Upregulated expression of cell–cell adhesion molecules, including cadherins and selectins, facilitates leukocyte binding to the endothelium, further compromising the glycocalyx and augmenting vascular permeability<sup>35,36</sup>. The complement system, an integral component of the innate immune response, is also activated in sepsis. Its activation results in the production of factors that enhance endothelial expression of adhesion molecules, thereby increasing vascular permeability<sup>37</sup>. Complement-mediated cleavage of glycocalyx components exacerbates barrier dysfunction<sup>38</sup>. The aforementioned biological processes are closely associated with endothelial function and vascular barrier integrity. Disruptions therein can precipitate heightened vascular permeability and glycocalyx injury, which are pivotal in the pathogenesis of sepsis and its clinical sequelae. These findings underscore the complex interplay between gene expression, endothelial biology, and the hemodynamic perturbations observed in septic patients.

Genes chosen to construct the benefit scores encompass both protein-coding and non-coding genes, with regulatory mechanisms too intricate for our study's scope. Given that proteins serve as the ultimate effectors, utilizing plasma protein levels may offer greater biological relevance for recommending fluid strategies. The proteins comprising our proteomic signature are biologically explicable. For instance, CSF3 regulates the production, differentiation, and function of granulocytes, innate immune cells crucial for immune response<sup>39,40</sup>. This protein is commonly used to manage chemotherapy-induced neutropenia. Granulocytes also release vasodilatory mediators contributing to septic shock, wherein a liberal fluid strategy aids in restoring effective circulatory volume. Hence, higher CSF3 values are associated with increased benefits from a liberal fluid strategy.

Several study limitations warrant acknowledgment. Firstly, A critical consideration in our study design was the categorization of fluid strategies. While this approach has the advantage of providing clear categorization for analysis, it also introduces potential limitations. The choice of the 3000 ml threshold and the SOFA<sub>cv</sub> score cutoff are based on clinical judgment and existing literature, which may not be universally applicable across all patient populations or settings. Furthermore, the categorization may not fully capture the complexity and individual variability in clinical decision-making regarding fluid management. The potential for variability in fluid strategy application could introduce bias or confounding in our analysis. Additionally, the observational nature of our study and reliance on recorded data means that we cannot account for all the nuances and rationale behind fluid management decisions made by treating physicians. Future studies with a prospective design, standardized fluid management protocols, and a larger and more diverse patient population are needed to validate and refine our approach. Secondly, the relative protein values utilized in the study necessitate batch normalization, highlighting the need for validation of the proteomic signature's accuracy through

ELISA-tested plasma protein concentrations. We also acknowledge that the current assays for GAL, NFASC, MAP2K6, and others do not provide results within the immediate timeframes (<1 h) required for ICU resuscitation. This limitation underscores the need for the development of rapid diagnostic tools, which is a critical area for future research. In the current study, one limitation is the absence of data regarding the specific types of fluids used for resuscitation, be it balanced or unbalanced. The choice of fluid can potentially influence clinical outcomes, particularly in the context of sepsis, where fluid management is a critical component of treatment<sup>41,42</sup>. While our analysis did not account for this variable, we acknowledge that the type of fluid may play a pivotal role in patient responses and survival, especially considering the evolving understanding of sepsis subphenotypes and their tailored management strategies<sup>43</sup>. While the findings of this study provide valuable insights into individualized fluid strategy, it is important to recognize that our results are primarily applicable to patients whose data closely resemble those in our training set. The generalizability of these results to other populations or settings may be limited due to differences in patient demographics, comorbidities, and clinical practices. Future studies are needed to validate the model's performance in diverse populations and to explore its applicability in different clinical scenarios.

To effectively translate our findings into clinical practice, several pivotal steps must be undertaken. Firstly, we must subject our model to prospective validation to ensure its predictive accuracy in diverse patient populations. Secondly, the development of rapid and sensitive assays for the identified proteomic signature is essential for practical clinical application. Lastly, a cost-effectiveness analysis will assess the economic viability of our approach, considering both direct costs and potential savings from improved patient outcomes.

In conclusion, this study presents a proteomic signature with potential applications in guiding fluid strategy for patients with septic shock. However, further validation studies are necessary to establish the causal relationship between fluid strategy and survival outcomes.

## Methods

### Study setting and patient enrollment

The study received approval from the ethics committee of Sir Run Run Shaw Hospital (approval number: 20201014-39), and written informed consent was obtained from patients or their next-of-kin surrogates. Participants received non-monetary compensation in the form of access to their personal data, providing potential insights into their health and personalized recommendations. Conducted within the Chinese Multi-omics Advances In Sepsis (CMAISE) consortium between November 2020 and December 2023, this study involved 35 Chinese hospitals<sup>44</sup>. The study protocol was registered with the Chinese Clinical Trial Registry (<http://www.chictr.org.cn/>; ChiCTR2000040446)<sup>45</sup>. Patient eligibility was based on meeting the Sepsis-3.0 criteria (suspected or documented infection plus acute increase in SOFA score > 2 points) upon admission to the intensive care unit (ICU)<sup>46</sup>. Septic shock was defined as those with hypotension (mean arterial pressure <65 mmHg) requiring vasopressors despite adequate fluid resuscitation. Exclusion criteria included: (1) end-stage cirrhosis with Child–Pugh C; (2) concomitant malignancy or autoimmune disease; (3) do-not-resuscitate order; (4) pregnancy; (5) sepsis



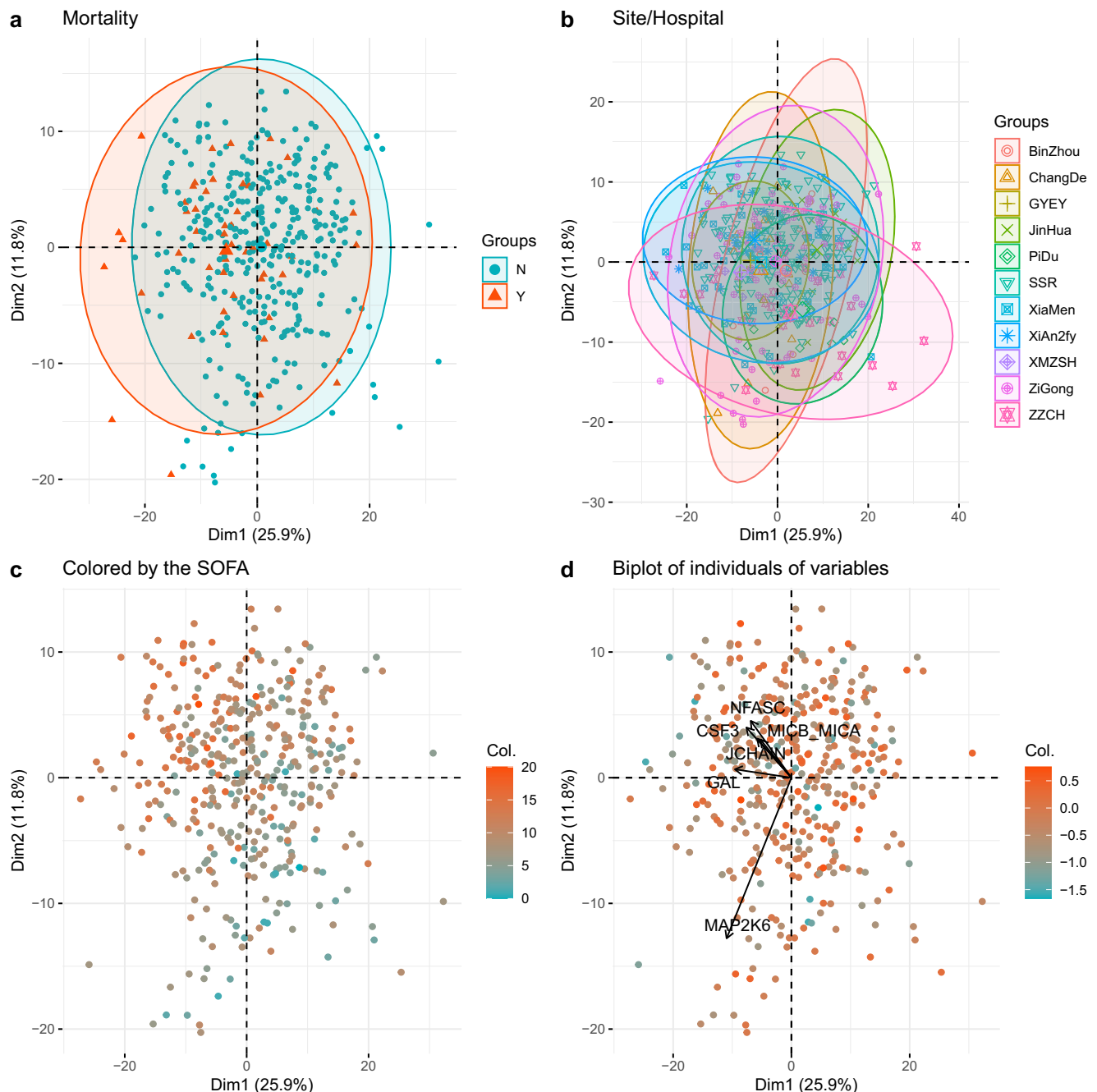


**Fig. 6 | Principal component analysis (PCA) biplot of protein expression profiles by clinical, biological, and technical variables.** These dimension reduction plots present the results of a PCA on protein expression data, illustrating the variance in protein expression across different clinical, biological, and technical variables. The first two principal components, Dim1 and Dim2, account for 25.9% and 11.8% of the total variance, respectively (a). PCA Biplot colored by mortality status, highlighting the separation between Survivors (Y) and non-survivors (N). The projection of individual data points shows the distribution of samples along the principal components, with color intensity indicating the presence of mortality (b). PCA Biplot differentiated by site/hospital. Each site/hospital is represented by a distinct symbol, demonstrating the clustering and dispersion of samples based on their protein expression profiles (c). PCA Biplot colored by the SOFA score, a measure of organ dysfunction. The gradient from light to dark represents increasing SOFA scores, reflecting the severity of organ failure in the samples (d).

Close-up view of the PCA biplot focusing on the individual variables (proteins) GAL, NFASC, MICB\_MICA, MAP2K6, JCHAIN, and CSF3. The arrows represent the direction and magnitude of the contribution of each protein to the principal components. The angle and length of these arrows indicate the correlation of each protein with the principal components. The color gradient from blue to red on the visualization indicates escalating benefit scores, with blue representing lower scores and red indicating higher, positive values that suggest a beneficial response to restrictive fluid strategies. CSF3 colony-stimulating factor 3, GAL galanin, NFASC neurofascin, MICB\_MICA MHC class I polypeptide-related sequence B and MICA, MAP2K6 mitogen-activated protein kinase kinase 6, JCHAIN joining chain of multi-meric IgA and IgM, SOFA sequential organ failure assessment, PCA principal component analysis, Dim1 dimension 1, Dim2 dimension 2, N no, Y yes, BinZhou, ChangDe, GYY, JinHua, PiDu, SSR, XiaMen, XiAn2fy, XMZSH, ZiGong, ZZCH site or hospital identifiers.

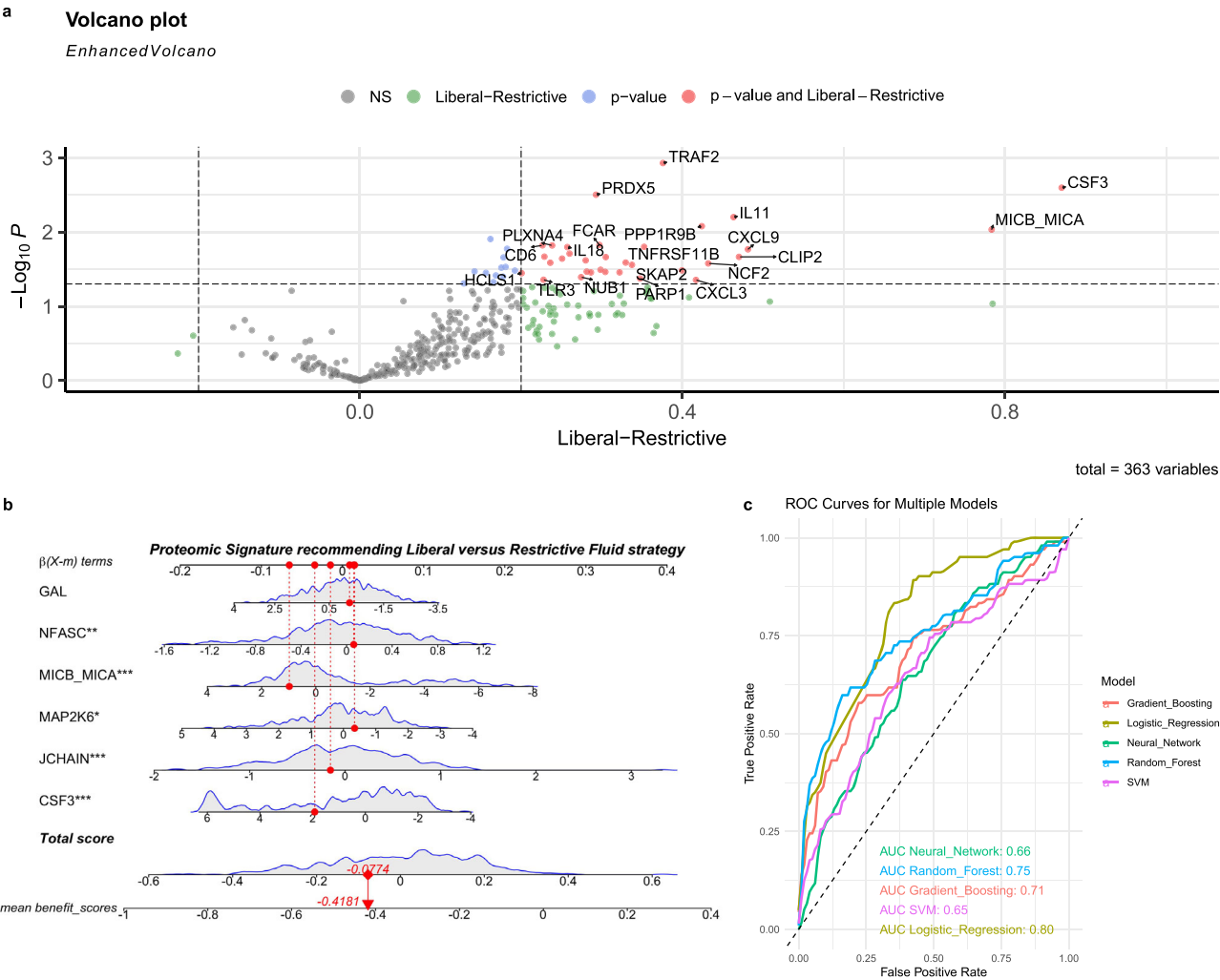


**Fig. 7 | Development of a protein signature model for recommending liberal or restrictive fluid strategy.** **a** Comparative analysis of plasma protein expression levels between the restrictive ( $n = 102$  person-days) and liberal ( $n = 311$  person-days) fluid strategy cohorts. Two-sided  $p$ -values were adjusted using the Benjamini–Hochberg procedure. **b** Nomogram demonstrating the estimation of benefit scores based on plasma protein levels. The red lines represent a sample

patient, with a score of  $-0.42$ , suggesting potential benefit from the liberal strategy. Two-sided  $p$ -values are reported for each variable; Significance levels are indicated with asterisks as follows:  $p < 0.05$ ,  $^{**}p < 0.01$ , and  $^{***}p < 0.005$ . **c** ROC plot illustrating the diagnostic accuracy of the protein signature for identifying patients who may benefit from the restrictive fluid strategy.

onset  $> 48$  h or treatment at other hospitals when presenting to CMAISE member hospitals; (6) immunosuppression, such as long-term use of immunosuppressive agents, chemotherapy, corticosteroids, radiotherapy, or HIV infection; and (7) acute myocardial infarction

**Table 3 | Protein markers in the LASSO model for prediction of benefit score**

Proteins	Coefficient	CI	$p$
(Intercept)	$-0.34$	$[-0.38, -0.29]$	$<0.001$
CSF3	$-0.03$	$[-0.05, -0.01]$	$<0.001$
JCHAIN	$0.12$	$[0.05, 0.19]$	$0.001$
MAP2K6	$-0.04$	$[-0.07, -0.01]$	$0.025$
MICB_MICA	$-0.03$	$[-0.05, -0.02]$	$<0.001$
NFASC	$0.14$	$[0.05, 0.23]$	$0.002$
GAL	$-0.03$	$[-0.07, 0.01]$	$0.104$

Two-sided  $p$ -values are reported.  
GAL galanin and GMAP prepropeptide, NFASC neurofascin, MICB\_MICA MHC class I polypeptide-related sequence B and A, MAP2K6 mitogen-activated protein kinase 6, JCHAIN joining the chain of multimeric IgA and IgM, CSF3 colony-stimulating factor 3.

and/or pulmonary embolism. The inclusion criteria were designed to ensure a representative sample across various demographic factors, including sex and age.

### Blood sample preparation and testing

Blood samples were collected on days 1, 3, and 5, with peripheral whole blood samples obtained using PAXgene tubes and subsequently stored at  $-80^{\circ}\text{C}$ . These samples underwent library preparation and gene expression quantification by LC-Bio Technologies (Hangzhou) Co., LTD. The DESeq2 pipeline was utilized for differential gene expression analysis, with genes having less than 100 counts in all samples being excluded<sup>47</sup>. A variance stabilizing transformation (VST) was applied to normalize the count data, resulting in a homoscedastic matrix of values across the range of mean values. Batch effects originating from different institutions were mitigated using a design matrix incorporating sample source information. Differential gene expression between restrictive vs liberal strategy groups was depicted using volcano plots. Additionally, GSEA utilizing gene ontology (GO) terms was performed with the clusterProfiler package (version 4.12.0)<sup>48</sup>, to assist in deciphering the biological significance of the differentially expressed genes. This approach is crucial for understanding the broader

functional implications of the observed gene expression changes within our study<sup>49–51</sup>.

The Olink® inflammation panel (Olink Proteomics AB, Uppsala, Sweden) was utilized for protein quantification in accordance with the manufacturer's instructions. The protocol relies on the proximity extension assay (PEA) technology, wherein pairs of oligonucleotide-labeled antibody probes selectively bind to target proteins<sup>52</sup>. Upon close proximity, these probe pairs undergo pair-wise hybridization of the associated oligonucleotides. The subsequent introduction of a DNA polymerase initiates proximity-dependent DNA polymerization, resulting in the formation of a distinct PCR target sequence. This DNA sequence is then detected and quantified using a cutting-edge microfluidic real-time PCR instrument (Signature Q100, LC-Bio Technology CO., Ltd., Hangzhou, China). Subsequent analyses, including differential and enrichment analyses, were carried out following established protocols. Specifically, gene set enrichment analysis (GSEA)<sup>48</sup> was conducted using the Molecular Signatures Database (MSigDb)<sup>53,54</sup> and executed with the clusterProfiler R package (version 4.12.0).

### Important clinical variables and definitions

Upon admission, demographic information such as age, sex (based on hospital records), height, and weight were recorded as described previously. Laboratory parameters, including C-reactive protein, serum creatinine, urine output, procalcitonin, and coagulation profiles, were evaluated on days 1, 3, and 5. Fluid intake was documented on days 1, 3, and 5.

In our study, patients with septic shock were categorized into two groups based on their fluid management strategy: restrictive and liberal. The 'restrictive fluid strategy' was defined by two criteria: a SOFA cardiovascular score (SOFA\_cv) greater than 2 points, indicating a priority for vasopressor use, and a daily fluid intake of less than 3000 ml. Conversely, a 'liberal fluid strategy' was characterized by either a SOFA\_cv score of 2 points or less, or a daily fluid intake of 3000 ml or more.

The selection of the 3000 ml threshold for daily fluid intake was informed by a review of existing literature<sup>7,11,55,56</sup>, and aimed to ensure a sufficient number of patients in each group for robust statistical analysis and to allow for the identification of distinct subgroups within the septic shock population that might respond differently to fluid management strategies. The fluid strategy was assessed on days 1, 3, and 5 of the study period, capturing the initial and critical phase of septic shock treatment known to impact patient outcomes.

### Identification of subgroups showing differential responses to the fluid strategy

The analysis pipeline included four steps: (1) create a propensity score function and assess the diagnostics of the propensity scores. (2) Select and train a model for subgroup identification. (3) Compute the treatment effects within the identified subgroups. (4) Visualize and analyze the treatment effects of the model and subgroups<sup>57</sup>. Essentially, we want to see if treatment affects patients' outcomes differently. We consider patient characteristics (whole blood transcriptome), treatment status (liberal vs restrictive strategy), and the outcome of interest (survival outcome). The main goal is to estimate a "benefit score" for each patient, which tells us how much they're expected to benefit from treatment. If the score is positive, the treatment is likely beneficial for them; if it's negative or zero, the control might be better. This helps us identify which patients benefit from treatment<sup>58</sup>.

Validation of the model was conducted in a separate cohort that did not overlap with the original one. The validation data was withheld during model development and the analysts were blinded to the validation dataset throughout the model building process. The validation of our model was performed independently by a statistician who was not involved in the training of the model. In this new cohort, we computed a "benefit score" for each patient, where higher scores

suggested a higher likelihood of recommending a restrictive fluid strategy. The objective was to determine whether patients with congruent recommended and administered fluid strategies exhibited superior survival outcomes compared to those with disparate strategies. Given that patients were followed and had blood samples collected for transcriptome and proteomics analysis on days 1, 3, and 5, we recognized the need to account for changes in patient status and biomarker levels over time. The time-varying nature of these covariates necessitated the use of a Cox model that could accommodate such changes<sup>59,60</sup>. This approach allows for the incorporation of time-dependent covariates, reflecting the dynamic nature of the clinical course in sepsis patients.

### Proteomic signature to facilitate clinical translation

To enhance clinical translation, we focused on developing a proteomic signature. Plasma proteins offer greater stability compared to transcriptome data and exhibit strong correlations with clinical chemistry parameters<sup>61</sup>. Leveraging this connection, we aimed to create a signature capable of identifying patient subgroups benefiting from either liberal or restrictive fluid strategies. Using the Least Absolute Shrinkage and Selection Operator (LASSO)<sup>62</sup>, we filtered significant proteins from a pool of 363 plasma proteins. Subsequently, we constructed a nomogram for a simplified clinical application of the subgroup prediction model (Fig. 1). The efficacy of the model in terms of predictive accuracy was determined by calculating the area under the receiver operating characteristic (ROC) curve. To ascertain the precision of this estimate, a non-parametric bootstrap technique was employed for calculating the 95% CI for the AUC. This approach, known for its robustness, involves resampling the data with replacement to generate an empirical distribution of AUCs from which the CI is derived. To ensure robustness, prevent overfitting, and enhance the generalizability of the findings, multiple models were evaluated, including support vector machine (SVM), random forest, neural networks, and gradient boosting. This evaluation aimed to determine whether these models offer significant improvement over the logistic regression model. Default settings in the parsnip package (v1.2.1) were employed for training these models.

### Reporting summary

Further information on research design is available in the Nature Portfolio Reporting Summary linked to this article.

### Data availability

The transcriptomic data generated in this study have been deposited in the National Genomic Data Center database under accession number [PRJCA006118](https://ngdc.cncb.ac.cn/prj/PRJCA006118). The raw transcriptomic data are available under restricted access for regulatory laws of our country, access can be obtained by formal approval from the National Genomic Data Center. Access requests for the transcriptomics data at PRJCA006118 will typically be processed within 2 weeks. The raw patient individual data are protected and are not available due to data privacy laws. The processed transcriptomic data are available at <https://ngdc.cncb.ac.cn/omix/release/OMIX006457>. The proteomic data generated in this study are provided in the National Genomic Data Center database under accession number [OMIX006238](https://ngdc.cncb.ac.cn/omix/release/OMIX006238). The "minimum dataset" that is necessary to interpret, verify, and extend the research in this article is included in the manuscript and its supplementary information. Source data are provided with this paper. For a more detailed description of the data, please visit the CMAISE project page (<https://github.com/zh-zhang1984/CMAISE/wiki>). Source data are provided with this paper.

### References

- Gendreau, S. et al. Geo-economic influence on the effect of fluid volume for sepsis resuscitation: a meta-analysis. *Am. J. Respir. Crit. Care Med.* **209**, 517–528 (2024).

2. De Backer, D. et al. How can assessing hemodynamics help to assess volume status? *Intensive Care Med.* **48**, 1482–1494 (2022).
3. Zampieri, F. G., Bagshaw, S. M. & Semler, M. W. Fluid therapy for critically ill adults with sepsis: a review. *JAMA* **329**, 1967–1980 (2023).
4. Bissell, B. D. & Mefford, B. Pathophysiology of volume administration in septic shock and the role of the clinical pharmacist. *Ann. Pharmacother.* **54**, 388–396 (2020).
5. Self, W. H. et al. Liberal versus restrictive intravenous fluid therapy for early septic shock: rationale for a randomized trial. *Ann. Emerg. Med.* **72**, 457–466 (2018).
6. Keijzers, G. et al. The Australasian resuscitation in sepsis evaluation: fluids or vasopressors in emergency department sepsis (ARISE FLUIDS), a multi-centre observational study describing current practice in Australia and New Zealand. *Emerg. Med. Australas.* **32**, 586–598 (2020).
7. Meyhoff, T. S. et al. Restriction of intravenous fluid in ICU patients with septic shock. *N. Engl. J. Med.* **386**, 2459–2470 (2022).
8. Sivapalan, P. et al. Restrictive versus standard IV fluid therapy in adult ICU patients with septic shock-Bayesian analyses of the CLASSIC trial. *Acta Anaesthesiol. Scand.* **68**, 236–246 (2024).
9. National Heart, Lung, and Blood Institute Prevention and Early Treatment of Acute Lung Injury Clinical Trials Network et al. Early restrictive or liberal fluid management for sepsis-induced hypotension. *N. Engl. J. Med.* **388**, 499–510 (2023).
10. Andrews, B. et al. Effect of an early resuscitation protocol on in-hospital mortality among adults with sepsis and hypotension: a randomized clinical trial. *JAMA* **318**, 1233–1240 (2017).
11. Macdonald, S. P. J. et al. Restricted fluid resuscitation in suspected sepsis associated hypotension (REFRESH): a pilot randomised controlled trial. *Intensive Care Med.* **44**, 2070–2078 (2018).
12. Myles, P. S. et al. Restrictive versus liberal fluid therapy for major abdominal surgery. *N. Engl. J. Med.* **378**, 2263–2274 (2018).
13. Kjær, M.-B. N. et al. Long-term effects of restriction of intravenous fluid in adult ICU patients with septic shock. *Intensive Care Med.* **49**, 820–830 (2023).
14. Shahnoor, H. et al. The effects of restrictive fluid resuscitation on the clinical outcomes in patients with sepsis or septic shock: a meta-analysis of randomized-controlled trials. *Cureus* **15**, e45620 (2023).
15. Vaeli Zadeh, A., Wong, A., Crawford, A. C., Collado, E. & Larned, J. M. Guideline-based and restricted fluid resuscitation strategy in sepsis patients with heart failure: a systematic review and meta-analysis. *Am. J. Emerg. Med.* **73**, 34–39 (2023).
16. Wong, H. R. et al. Combining prognostic and predictive enrichment strategies to identify children with septic shock responsive to corticosteroids. *Crit. Care Med.* **44**, e1000–e1003 (2016).
17. Antcliffe, D. B. et al. Transcriptomic signatures in sepsis and a differential response to steroids. From the VANISH randomized trial. *Am. J. Respir. Crit. Care Med.* **199**, 980–986 (2019).
18. Sweeney, T. E. et al. A community approach to mortality prediction in sepsis via gene expression analysis. *Nat. Commun.* **9**, 694 (2018).
19. Sun, W. et al. Disruption of pulmonary microvascular endothelial barrier by dysregulated claudin-8 and claudin-4: uncovered mechanisms in porcine reproductive and respiratory syndrome virus infection. *Cell Mol. Life Sci.* **81**, 240 (2024).
20. Sun, Z. et al. PRRSV-induced inflammation in pulmonary intravascular macrophages (PIMs) and pulmonary alveolar macrophages (PAMs) contributes to endothelial barrier function injury. *Vet. Microbiol.* **281**, 109730 (2023).
21. An, X. et al. A type 2 deiodinase-dependent increase in vegfa mediates myoblast-endothelial cell crosstalk during skeletal muscle regeneration. *Thyroid* **31**, 115–127 (2021).
22. Sabatino, L. et al. Thyroid hormone deiodinases D1, D2, and D3 are expressed in human endothelial dermal microvascular line: effects of thyroid hormones. *Mol. Cell Biochem.* **399**, 87–94 (2015).
23. Antcliffe, D. B. et al. Patient stratification using plasma cytokines and their regulators in sepsis: relationship to outcomes, treatment effect and leucocyte transcriptomic subphenotypes. *Thorax*. <https://doi.org/10.1136/thorax-2023-220538> (2024).
24. Davenport, E. E. et al. Genomic landscape of the individual host response and outcomes in sepsis: a prospective cohort study. *Lancet Respir. Med.* **4**, 259–271 (2016).
25. Scicluna, B. P. et al. Classification of patients with sepsis according to blood genomic endotype: a prospective cohort study. *Lancet Respir. Med.* **5**, 816–826 (2017).
26. Cui, M., Cheng, C. & Zhang, L. High-throughput proteomics: a methodological mini-review. *Lab Invest.* **102**, 1170–1181 (2022).
27. Souchak, J., Mohammed, N. B. B., Lau, L. S. & Dimitroff, C. J. The role of galectins in mediating the adhesion of circulating cells to vascular endothelium. *Front Immunol.* **15**, 1395714 (2024).
28. Machino, T. et al. Apoptosis signal-regulating kinase 1-mediated signaling pathway regulates hydrogen peroxide-induced apoptosis in human pulmonary vascular endothelial cells. *Crit. Care Med.* **31**, 2776–2781 (2003).
29. Abdelbaky, A. M., Elmasry, W. G. & Awad, A. H. Restrictive versus liberal fluid regimen in refractory sepsis and septic shock: a systematic review and meta-analysis. *Cureus* **15**, e47783 (2023).
30. Shankar-Hari, M. et al. Reframing sepsis immunobiology for translation: towards informative subtyping and targeted immunomodulatory therapies. *Lancet Respir. Med.* [https://doi.org/10.1016/S2213-2600\(23\)00468-X](https://doi.org/10.1016/S2213-2600(23)00468-X) (2024).
31. Reddy, K. et al. Subphenotypes in critical care: translation into clinical practice. *Lancet Respir. Med.* **8**, 631–643 (2020).
32. Zhang, Z. et al. Deep learning-based clustering robustly identified two classes of sepsis with both prognostic and predictive values. *EBioMedicine* **62**, 103081 (2020).
33. Berger, J. O., Wang, X. & Shen, L. A Bayesian approach to subgroup identification. *J. Biopharm. Stat.* **24**, 110–129 (2014).
34. Lipkovich, I., Dmitrienko, A. & B, R. Tutorial in biostatistics: data-driven subgroup identification and analysis in clinical trials. *Stat. Med.* **36**, 136–196 (2017).
35. Gamble, J. R. et al. Angiopoietin-1 is an antipermeability and anti-inflammatory agent in vitro and targets cell junctions. *Circ. Res.* **87**, 603–607 (2000).
36. Rho, S.-S., Ando, K. & Fukuhara, S. Dynamic regulation of vascular permeability by vascular endothelial cadherin-mediated endothelial cell–cell junctions. *J. Nippon Med. Sch.* **84**, 148–159 (2017).
37. Langston, J. C. et al. Omics of endothelial cell dysfunction in sepsis. *Vasc. Biol.* **4**, R15–R34 (2022).
38. van der Poll, T. & Parker, R. I. Platelet activation and endothelial cell dysfunction. *Crit. Care Clin.* **36**, 233–253 (2020).
39. Dong, J., Wang, S., Hu, Z. & Gong, L. Extracellular proteins as potential biomarkers in sepsis-related cerebral injury. *Front. Immunol.* **14**, 1128476 (2023).
40. Wilhelmssen, K., Mesa, K. R., Prakash, A., Xu, F. & Hellman, J. Activation of endothelial TLR2 by bacterial lipoprotein upregulates proteins specific for the neutrophil response. *Innate Immun.* **18**, 602–616 (2012).
41. Zhang, J. et al. ACETATE RINGER'S SOLUTION VERSUS NORMAL SALINE SOLUTION IN SEPSIS: A RANDOMIZED, CONTROLLED TRIAL. *Shock* **61**, 520–526 (2024).
42. Rochwerf, B. et al. Fluid resuscitation in sepsis: a systematic review and network meta-analysis. *Ann. Intern Med.* **161**, 347–355 (2014).
43. Scherger, S. J. & Kalil, A. C. Sepsis phenotypes, subphenotypes, and endotypes: are they ready for bedside care? *Curr. Opin. Crit. Care*. <https://doi.org/10.1097/MCC.0000000000001178> (2024).



44. Zhang, Z. zh-zhang1984/CMAISE: identifying septic shock sub-groups to tailor fluid strategies through multi-omics integration. Zenodo <https://doi.org/10.5281/zenodo.13689848> (2024).
45. Zhang, Z. et al. Gene signature for the prediction of the trajectories of sepsis-induced acute kidney injury. *Crit. Care* **26**, 398 (2022).
46. Singer, M. et al. The third international consensus definitions for sepsis and septic shock (sepsis-3). *JAMA* **315**, 801–810 (2016).
47. Love, M. I., Huber, W. & Anders, S. Moderated estimation of fold change and dispersion for RNA-seq data with DESeq2. *Genome Biol.* **15**, 550 (2014).
48. Subramanian, A. et al. Gene set enrichment analysis: a knowledge-based approach for interpreting genome-wide expression profiles. *Proc. Natl. Acad. Sci. USA* **102**, 15545–15550 (2005).
49. Gene Ontology Consortium. The gene ontology resource: enriching a GOld mine. *Nucleic Acids Res.* **49**, D325–D334 (2021).
50. Wu, T. et al. clusterProfiler 4.0: a universal enrichment tool for interpreting omics data. *Innovation* **2**, 100141 (2021).
51. Ashburner, M. et al. Gene ontology: tool for the unification of biology. *Nat. Genet.* **25**, 25–29 (2000).
52. Wik, L. et al. Proximity extension assay in combination with next-generation sequencing for high-throughput proteome-wide analysis. *Mol. Cell Proteom.* **20**, 100168 (2021).
53. Liberzon, A. et al. Molecular signatures database (MSigDB) 3.0. *Bioinformatics* **27**, 1739–1740 (2011).
54. Liberzon, A. et al. The molecular signatures database (MSigDB) hallmark gene set collection. *Cell Syst.* **1**, 417–425 (2015).
55. Corl, K. A. et al. The restrictive IV fluid trial in severe sepsis and septic shock (RIFTS): a randomized pilot Study. *Crit. Care Med.* **47**, 951–959 (2019).
56. Semler, M. W., Janz, D. R., Casey, J. D., Self, W. H. & Rice, T. W. Conservative Fluid Management After Sepsis Resuscitation: A Pilot Randomized Trial. *J. Intensive Care Med.* **35**, 1374–1382 (2020).
57. Chen, S., Tian, L., Cai, T. & Yu, M. A general statistical framework for subgroup identification and comparative treatment scoring. *Bio-metrics* **73**, 1199–1209 (2017).
58. Huling, J. D. & Yu, M. Subgroup identification using the personalized package. *J. Stat. Soft.* **98**, 1–60 (2021).
59. Fisher, L. D. & Lin, D. Y. Time-dependent covariates in the Cox proportional-hazards regression model. *Annu. Rev. Public Health* **20**, 145–157 (1999).
60. Zhang, Z., Reinikainen, J., Adeleke, K. A., Pieterse, M. E. & Groothuis-Oudshoorn, C. G. M. Time-varying covariates and coefficients in Cox regression models. *Ann. Transl. Med.* **6**, 121 (2018).
61. Tebani, A. et al. Integration of molecular profiles in a longitudinal wellness profiling cohort. *Nat. Commun.* **11**, 4487 (2020).
62. Tibshirani, R. Regression shrinkage and selection via the lasso. *J. Royal Stat Soc B* **58**, 267–288 (1996).

## Acknowledgements

The study was supported by funding from the China National Key Research and Development Program (no. 2023YFC3603104, Z.Z.), the National Natural Science Foundation of China (82272180, Z.Z.), the Huadong Medicine Joint Funds of the Zhejiang Provincial Natural Science Foundation of China under grant no. LHDMD24H150001 (Z.Z.). A collaborative scientific project co-established by the Science and Technology Department of the National Administration of Traditional Chinese Medicine and the Zhejiang Provincial Administration of

Traditional Chinese Medicine (GZY-ZJ-KJ-24082, Z.Z.), General Health Science and Technology Program of Zhejiang Province (2024KY1099, Z.Z.). Key Project of Jinhua City (2022-3-102, 2023-1-099, 2022-3-092, 2023-3-90, and 2023-3-092, L.C.), National Natural Science Foundation of China (82260373, S.C.), Hainan Province Science and Technology Special Fund (ZDKJ2021038, S.C.); Hainan Province Science and Technology Special Fund (ZDKJ2021038, S.Z.).

## Author contributions

L. Chen and Z. Zhang designed the study and drafted the manuscript; S.C., L.X., J.Y., B.Z., Y.H., P.X., and Z. Zhong helped interpret the results and write some discussions. L. Cheng and H.N. performed statistical analysis and result interpretation. B.S., Z.R., P.P., W.Z., X.J., B.W., and S.Z. performed subject enrollment and sample preparations. Z. Zhang is identified as the guarantor of the paper, taking responsibility for the integrity of the work as a whole, from inception to published article. All authors read and approved the final manuscript.

## Competing interests

There is no competing interest.

## Additional information

**Supplementary information** The online version contains supplementary material available at

<https://doi.org/10.1038/s41467-024-53239-9>.

**Correspondence** and requests for materials should be addressed to Zhongheng Zhang.

**Peer review information** *Nature Communications* thanks Natalja Stanski, and the other, anonymous, reviewers for their contribution to the peer review of this work. A peer review file is available.

**Reprints and permissions information** is available at <http://www.nature.com/reprints>

**Publisher's note** Springer Nature remains neutral with regard to jurisdictional claims in published maps and institutional affiliations.




**Open Access** This article is licensed under a Creative Commons Attribution-NonCommercial-NoDerivatives 4.0 International License, which permits any non-commercial use, sharing, distribution and reproduction in any medium or format, as long as you give appropriate credit to the original author(s) and the source, provide a link to the Creative Commons licence, and indicate if you modified the licensed material. You do not have permission under this licence to share adapted material derived from this article or parts of it. The images or other third party material in this article are included in the article's Creative Commons licence, unless indicated otherwise in a credit line to the material. If material is not included in the article's Creative Commons licence and your intended use is not permitted by statutory regulation or exceeds the permitted use, you will need to obtain permission directly from the copyright holder. To view a copy of this licence, visit <http://creativecommons.org/licenses/by-nc-nd/4.0/>.

© The Author(s) 2024

<sup>1</sup>Department of Emergency Medicine, Provincial Key Laboratory of Precise Diagnosis and Treatment of Abdominal Infection, Sir Run Run Shaw Hospital, Zhejiang University School of Medicine, Hangzhou, China. <sup>2</sup>School of Medicine, Shaoxing University, Shaoxing, People's Republic of China. <sup>3</sup>Department of Neurosurgery, Neurological Intensive Care Unit, Affiliated Jinhua Hospital, Zhejiang University School of Medicine, Jinhua, China. <sup>4</sup>Department of Emergency Medicine, Binzhou Medical University Hospital, Binzhou, People's Republic of China. <sup>5</sup>Department of Emergency, Third Affiliated Hospital, Wenzhou Medical University, Wenzhou, China. <sup>6</sup>College of Pulmonary & Critical Care Medicine, 8th Medical Center, Chinese PLA General Hospital, Beijing, China. <sup>7</sup>Intensive

Care Unit, Affiliated Dongyang Hospital of Wenzhou Medical University, Dongyang, Zhejiang, People's Republic of China. <sup>8</sup>Key Laboratory of Emergency and Trauma of Ministry of Education, Engineering Research Center for Hainan Biological Sample Resources of Major Diseases, Key Laboratory of Tropical Cardiovascular Diseases Research of Hainan Province, The First Affiliated Hospital of Hainan Medical University, Hainan, China. <sup>9</sup>Hainan Women and Children Medical Center, Hainan Medical University, Haikou, China. <sup>10</sup>Department of Wound Repair, Key Laboratory of Emergency and Trauma of Ministry of Education, The First Affiliated Hospital of Hainan Medical University, Haikou, China. <sup>11</sup>Department of Intensive Care Unit, The First Affiliated Hospital of Hainan Medical University, Haikou, China. <sup>12</sup>Department of Pathology, The Second Affiliated Hospital of Hainan Medical University, Haikou, China. <sup>13</sup>Emergency Department, Zigong Fourth People's Hospital, Zigong, China. <sup>14</sup>Department of Critical Care Medicine, Affiliated Jinhua Hospital, Zhejiang University School of Medicine, Jinhua, China. <sup>15</sup>These authors contributed equally: Zhongheng Zhang, Lin Chen, Shaojiang Zheng, Shaowen Cheng. ✉ e-mail: [zh\\_zhang1984@zju.edu.cn](mailto:zh_zhang1984@zju.edu.cn)

## the Chinese Multi-omics Advances In Sepsis (CMAISE) Consortium

**Zhongheng Zhang** <sup>1,2,15</sup> ✉, **Lin Chen**<sup>3,15</sup>, **Bin Sun**<sup>4</sup>, **Zhanwei Ruan**<sup>5</sup>, **Pan Pan**<sup>6</sup>, **Weimin Zhang**<sup>7</sup>, **Xuandong Jiang** <sup>7</sup>, **Shaojiang Zheng** <sup>8,9,15</sup>, **Shaowen Cheng**<sup>10,15</sup>, **Lina Xian**<sup>11</sup>, **Bingshu Wang**<sup>12</sup>, **Jie Yang**<sup>1</sup>, **Bo Zhang**<sup>1</sup>, **Ping Xu**<sup>13</sup>, **Zhitao Zhong**<sup>13</sup>, **Lingxia Cheng**<sup>13</sup>, **Hongying Ni**<sup>14</sup> & **Yucai Hong**<sup>1</sup>

A full list of members and their affiliations appears in the Supplementary Information.